

# Engineering Computations of Large Infrastructures in the Presence of Uncertainty

Achintya Haldar  
Department of Civil Engineering & Engineering Mechanics  
University of Arizona, Tucson, AZ 85721  
E-mail: haldar@u.arizona.edu

**Abstract:** Engineering computation capability has advanced exponentially in recent years. Increased computer power is one of the major reasons for this growth. It is now routine to incorporate sophisticated knowledge in computational schemes, but the presence of uncertainty must also be considered. Simulation-based schemes have been developed to address uncertainty-related problems. However, they have limited application to studying the realistic behavior of large infrastructure and the computations could be very tedious. The first part of the paper presents the incorporation of uncertainty in a finite element-based computational formulation to satisfy the underlying physics of large infrastructure, denoted as the stochastic finite element method. However, it becomes very inefficient when applied to time-domain dynamic problems. The concept is improved further by combining sensitivity analysis, model reduction techniques, efficient response surface method-based sampling schemes, and several advanced factorial schemes producing compounding beneficial effect to obtain efficiency without sacrificing accuracy. It is discussed in the second part. In the third part, sophisticated computation schemes are integrated with noise-contaminated measured response information to extract features of practical interest in the context of structural health assessment. The uncertainty in the measured data cannot completely be eliminated, but measured response data are needed to be integrated with advanced computational schemes for the maximum benefits. This is a very challenging task. In the late 1970s it was erroneously concluded that such integration was not possible, but the author and his team have proven otherwise.

**Keywords:** Reliability evaluation, implicit limit state function, stochastic finite element method, large infrastructures, nonlinear behavior, structural health assessment, noise-contaminated measured responses

## 1. Introduction

Conferences on Reliable Engineering Computing (REC) had a long history of cross-disciplinary theme integrating Civil/Mechanical Engineering, Computer Science, and Mathematics emphasizing basic research and developments and innovative applications. I feel privileged to be a part of it.

At the very beginning, it is important to differentiate between reliable computing and reliability-based computing. There may be very slight overlapping; however, in general they are different. Conceptually, reliable computing can be deterministic in formulation ignoring the presence of uncertainties in the problem. It is well known that the mathematical formulation itself is error prone since it is based on many assumptions and it is difficult to satisfy the underlying physics in most cases to track load path to failure. For large infrastructures, the mathematical formulations are extremely challenging. It is extremely difficult if not impossible to match computational predictions with experimental observations even for relatively

simple structures. Even if one ignores the uncertainty in the mathematical formulations, estimation of parameters to define the model is subject to various levels of uncertainty. If the response behavior is measured, it adds another layer of uncertainty. Even very sophisticated smart sensors are not totally error-free and experiments themselves are not completely reproducible.

The author initiated his research career by considering the presence of uncertainty in analytical engineering computing. He developed the stochastic finite element method (SFEM) to address the problem. He had to improve the concept to improve its efficiency so that it can be applied to very large systems. At present, his research includes structural health assessment using inversed algorithms to identify a system using noise-contaminated or uncertainty-filled measured response information. This is multi-disciplinary in nature and more demanding and challenging than developing SFEM. These areas are important in the context of engineering computation in the presence of uncertainty. They are briefly discussed in the paper.

## 2. Stochastic Finite Element Method

The applicability of reliability concept in analysis, design, and planning for infrastructures has been accepted by the engineering profession. Risk-based design has matured to the point that the information on risk alone is no longer sufficient; it is also necessary to know how accurately the information on uncertainty is incorporated in the mathematical formulation and the parameters to represent it. The first-generation design guidelines and codes have been modified or are being modified to reflect this concern.

Finite element analysis is a powerful tool commonly used by many engineering disciplines to analyze simple or complicated structures. It has matured significantly and has become routine to study behavior of structures as realistically as practicable considering complicated geometric arrangements, realistic connection and support conditions, various sources of nonlinearity and load path to failure for both static and dynamic applications of loadings. Most widely used reliability evaluation procedures failed to satisfy the above needs in most cases. On the other hand, the deterministic finite element method (FEM) fails to consider the presence of uncertainty in the formulations. Capturing the desirable features of both approaches, the author and his research team proposed the stochastic FEM or SFEM concept (Haldar and Mahadevan, 2000b). The probability of failure implies that it needs to be estimated just before failure satisfying physics-based complicated behavior. This indicates that a FEM-based general purpose reliability evaluation method, parallel to the deterministic analysis, is necessary and SFEM fills this vacuum.

### 2.1. Risk Estimation – Explicit Limit State Functions

Risk is always estimated with respect to limit state or performance functions. They are functions of all the random variables present in the formulation and the performance requirements satisfying the recommendation made in the design guidelines/codes or used in standard practices. Several methods with various degrees of sophistication are available (Haldar and Mahadevan, 2000a) for risk estimation. Most commonly used procedures are the first-order and second-order reliability methods (FORM/SORM). These algorithms are iterative in nature and the gradients of limit state functions are required to estimate the coordinates of the most probable failure point (MPFP), the corresponding reliability index, and the failure probability. However, since the explicit expression for a limit state function is not available for most structures of practical interest, their applications to estimate risk are very limited. For large infrastructures, limit state functions are implicit and calculations of gradients become challenging and complicated. This statement is also valid for relatively simpler nonlinear structures represented by finite elements.

## 2.2. Risk Estimation – Implicit Limit State Functions

For implicit limit state functions, several computational strategies can be followed. For this discussion, they can be broadly divided into three categories; (1) Monte Carlo simulation (MCS), (2) response surface method (RSM)-based approaches, and (3) sensitivity-based analysis. The basic MCS scheme could be simple to apply but could be inefficient, time-consuming, and impractical if the structure is represented with numerous finite elements and the deterministic solution takes a lot of time. The RSM-based approaches approximately construct the limit state function with the help of a few selected deterministic analyses. However, its applicability could be limited if the region where the limit state function needs to be generated is not known (Huh and Haldar, 2011). In the sensitivity-based approach, the sensitivity of the structural response to the input variables is computed and it can be integrated with the FORM/SORM approaches to extract the underlying reliability information. The value of the performance function is evaluated using deterministic structural analysis and the gradient is computed using sensitivity analysis. The concept can be implemented in three different ways: (1) through a finite difference approach, (2) through classical perturbation methods that apply the chain rule of differentiation to finite element analysis, and (3) through iterative perturbation analysis techniques. The sensitivity-based reliability analysis approach is more elegant and in general more efficient than the simulation or response surface methods. Haldar and Mahadevan (2000b) suggested the use of the iterative perturbation technique in the context of the basic nonlinear SFEM-based algorithm. The concept can also be applied when the limit state is explicit in nature.

Without losing any generality, the limit state function can be expressed in terms of the set of basic random variables  $\mathbf{x}$  (e.g., loads, material properties and structural geometry), the set of displacements  $\mathbf{u}$  and the set of load effects  $\mathbf{s}$  (except the displacements) such as internal forces, stresses, etc. The displacement  $\mathbf{u} = \mathbf{Q}\mathbf{D}$ , where  $\mathbf{D}$  is the global displacement vector and  $\mathbf{Q}$  is a transformation matrix. The limit state function can be expressed as  $g(\mathbf{x}, \mathbf{u}, \mathbf{s}) = 0$ . For reliability computation, it is convenient to transform  $\mathbf{x}$  into the standard normal space  $\mathbf{y} = \mathbf{y}(\mathbf{x})$  such that the elements of  $\mathbf{y}$  are statistically independent and have a standard normal distribution. An iterative algorithm can be used to locate the MPFP on the limit state function using the first-order approximation. During each iteration, the structural response and its gradient vectors are calculated using FEMs. The following iteration scheme can be used for finding the coordinates of MPFP:

$$\mathbf{y}_{i+1} = \left[ \mathbf{y}_i^t \alpha_i + \frac{g(\mathbf{y}_i)}{|\nabla g(\mathbf{y}_i)|} \right] \alpha_i \quad (1)$$

where

$$\nabla g(\mathbf{y}) = \left[ \frac{\partial g(\mathbf{y})}{\partial y_1}, \dots, \frac{\partial g(\mathbf{y})}{\partial y_n} \right]^t \quad \text{and} \quad \alpha_i = - \frac{\nabla g(\mathbf{y}_i)}{|\nabla g(\mathbf{y}_i)|} \quad (2)$$

To implement the algorithm, the gradient  $\nabla g(\mathbf{y})$  of the limit state function in the standard normal space can be derived as (Haldar and Mahadevan, 2000b):

$$\nabla g(\mathbf{y}) = \left[ \frac{\partial g(\mathbf{y})}{\partial \mathbf{s}} \mathbf{J}_{s,x} + \left( \mathbf{Q} \frac{\partial g(\mathbf{y})}{\partial \mathbf{u}} + \frac{\partial g(\mathbf{y})}{\partial \mathbf{s}} \mathbf{J}_{s,D} \right) \mathbf{J}_{D,x} + \frac{\partial g(\mathbf{y})}{\partial \mathbf{x}} \right] \mathbf{J}_{y,x}^{-1} \quad (3)$$

where  $\mathbf{J}_{i,j}$ 's are the Jacobians of transformation (e.g.,  $\mathbf{J}_{s,x} = \partial \mathbf{s} / \partial \mathbf{x}$ ) and  $y_i$ 's are statistically independent random variables in the standard normal space. The evaluation of the quantities in Eq. (3) will depend on the problem under consideration (linear or nonlinear, two- or three-dimensional, etc.) and the performance functions used. The essential numerical aspect of SFEM is the evaluation of three partial derivatives,  $\partial g / \partial \mathbf{s}$ ,  $\partial g / \partial \mathbf{u}$ , and  $\partial g / \partial \mathbf{x}$ , and four Jacobians,  $\mathbf{J}_{s,x}$ ,  $\mathbf{J}_{s,D}$ ,  $\mathbf{J}_{D,x}$ , and  $\mathbf{J}_{y,x}$ . They can be evaluated by procedures suggested by Haldar and Mahadevan (2000b) for linear and nonlinear, two- or three-dimensional structures. Once the coordinates of the design point  $\mathbf{y}^*$  are evaluated with a preselected convergence criterion, the reliability index  $\beta$  can be evaluated as:

$$\beta = \sqrt{(\mathbf{y}^*)^t (\mathbf{y}^*)} \quad (4)$$

The probability of failure,  $P_f$ , can be calculated as:

$$P_f = \Phi(-\beta) = 1.0 - \Phi(\beta) \quad (5)$$

where  $\Phi$  is the standard normal cumulative distribution function. The author and his team published numerous papers to validate the above procedure.

### 2.3. Reliable or Realistic Engineering Computation

Reliable or realistic deterministic engineering computations will depend on the sophistication used in the FEM formulation to represent the structure, connections and supports conditions, the material behavior, different sources of energy dissipation, different sources of nonlinearity that may develop before failure, etc. The nature of sophistication used will also affect the reliability computation – a confluence of reliable and reliability-based engineering computation. It is a very difficult area and cannot be comprehensively addressed in this paper. However, to illustrate the challenges, the following discussions are made.

#### 2.3.1. Realistic representation of connections and implications on the reliability estimation

It has been accepted in the profession that all connections used in frames are flexible or partially restrained (PR) with different rigidities. However, in general they are assumed to be fully restrained (FR) in any FEM representation. Consideration of appropriate rigidities in connections will add a major source of nonlinearity in the formulation invalidating commonly used procedures to analyze the structure and a major source of energy dissipation for the dynamic including dynamic loadings. In general, the relationship between the moment  $M$ , transmitted by the connection, and the relative rotation angle  $\theta$  is used to represent the flexible behavior. Among the many alternatives (Richard model, piecewise linear model, polynomial model, exponential model, B-Spline model, etc.), the Richard four-parameter moment-rotation model is chosen here to represent the flexible behavior of a connection. It can be expressed as (Richard and Abbott, 1975):

$$M = \frac{(k - k_p)\theta}{\left(1 + \left|\frac{(k - k_p)\theta}{M_0}\right|^N\right)^{1/N}} + k_p \theta \quad (6)$$

where  $M$  and  $\theta$  are defined earlier,  $k$  is the initial stiffness,  $k_p$  is the plastic stiffness,  $M_0$  is the reference moment, and  $N$  is the curve shape parameter. These parameters are identified in Fig. 1.

Although an ordinary beam-column element is used to represent a PR connection element for numerical analyses, its stiffness needs to be updated at each iteration since the stiffness representing the partial rigidity depends on  $\theta$ . This can be accomplished by updating the Young's modulus as:

$$E_c(\theta) = \frac{l_c}{I_c} K_C(\theta) = \frac{l_c}{I_c} \frac{\partial M(\theta)}{\partial \theta} \quad (7)$$

where  $l_c$ ,  $I_c$ , and  $K_C(\theta)$  are the length, the moment of inertia, and the tangent stiffness of the connection element, respectively.  $K_C(\theta)$  is calculated using Eq. (6) and can be shown to be:

$$K_C(\theta) = \frac{dM}{d\theta} = \frac{(k - k_p)}{\left(1 + \left|\frac{(k - k_p)\theta}{M_0}\right|^N\right)^{\frac{N+1}{N}}} + k_p \quad (8)$$

The Richard model discussed up to now represents only the monotonically increasing loading portion of the  $M$ - $\theta$  curves. However, the unloading and reloading behavior of the  $M$ - $\theta$  curves is also essential for any nonlinear seismic analysis. This subject was extensively addressed in the literature (Colson 1991, El-Salti 1992). They theoretically developed the unloading and reloading parts of the  $M$ - $\theta$  curves using the Masing rule. A general class of Masing models can be defined with a virgin loading curve expressed as:

$$f(M, \theta) = 0 \quad (9)$$

and its unloading and reloading curve can be described by the following equation:

$$f\left(\frac{M - M_a}{2}, \frac{\theta - \theta_a}{2}\right) = 0 \quad (10)$$

where  $(M_a, \theta_a)$  is the load reversal point as shown in Fig. 1.

Using the Masing rule and the Richard model represented by Eqs. (6) and (8), the unloading and reloading behavior of a PR connection can be generated as:

$$M = M_a - \frac{(k - k_p)(\theta_a - \theta)}{\left(1 + \left|\frac{(k - k_p)(\theta_a - \theta)}{2M_0}\right|^N\right)^{\frac{1}{N}}} - k_p(\theta_a - \theta) \quad (11)$$

and

$$K_c(\theta) = \frac{dM}{d\theta} = \frac{(k - k_p)}{\left(1 + \left|\frac{(k - k_p)(\theta_a - \theta)}{2M_0}\right|^N\right)^{\frac{N+1}{N}}} + k_p \quad (12)$$

If  $(M_b, \theta_b)$  is the next load reversal point, as shown in Fig. 1, the reloading relation between  $M$  and  $\theta$  can be obtained by simply replacing  $(M_a, \theta_a)$  with  $(M_b, \theta_b)$  in Eqs. (9) and (10). Thus, the proposed method uses Eqs. (6) and (8) when the connection is loading, and Eqs. (11) and (12) when the connection is unloading and reloading. This represents hysteretic behavior at the PR connections.

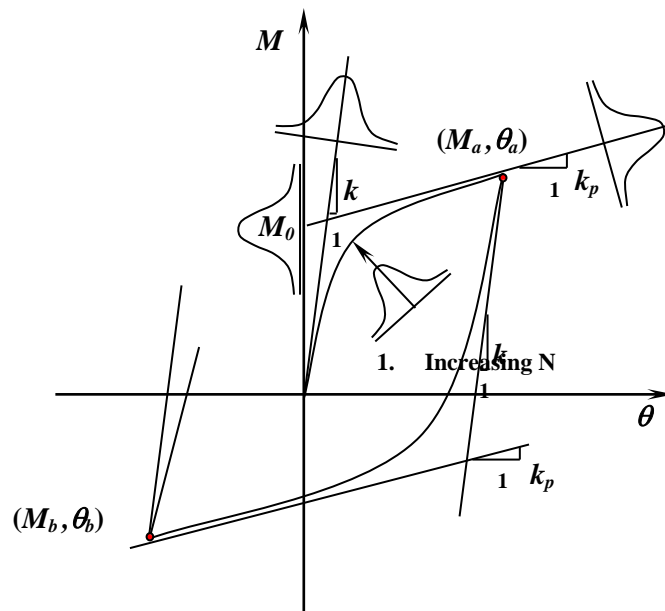


Figure 1.  $M$ - $\theta$  curve using the Richard Model, Masing rule and uncertainty (Huh & Haldar, 2002)

The basic FEM formulation of the structure remains unchanged, and thus the incorporation of the PR connection can be successfully accomplished. However, computational effort required is expected to be increased significantly. The consideration of appropriate connection rigidity is no longer an academic interest. During the Northridge earthquake of 1994, several connections in steel frames fractured in a brittle and premature manner. A typical connection, shown in Fig. 2, was fabricated with the beam flanges attached to the column flanges by full penetration welds (field-welded) and with the beam web bolted (field-bolted) to single plate shear tabs (Richard and Radau, 1998), denoted hereafter as the pre-NC.

In the post-Northridge design practices, the thrusts were to make the connections more flexible than the pre-NC and to move the location of formation of any plastic hinge away from the connection and to provide more ductility to increase the energy absorption capacity. Several improved connections can be found in the literature including cover plated connections, spliced beam connections, side-plated connections, bottom haunch connections, connections with vertical ribs, and connections with a reduced beam sections (RBS) or Dog-Boned (FEMA 350-3). Seismic Structural Design Associates, Inc. (SSDA) proposed a unique

proprietary slotted web (SSDA SlottedWeb™) moment connection (Richard et al. 1997), as shown in Fig. 3, denoted hereafter as the post-NC.

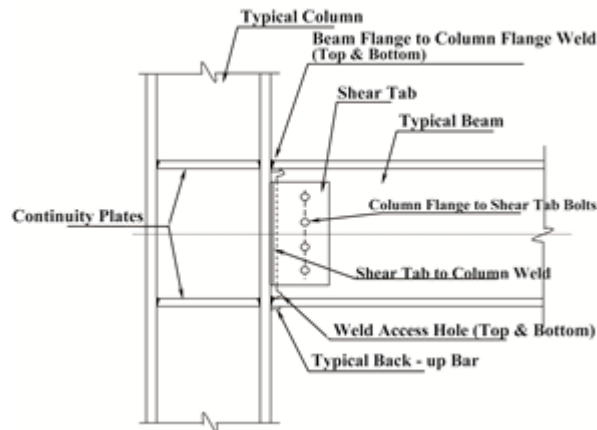


Figure 2. A typical pre-NC

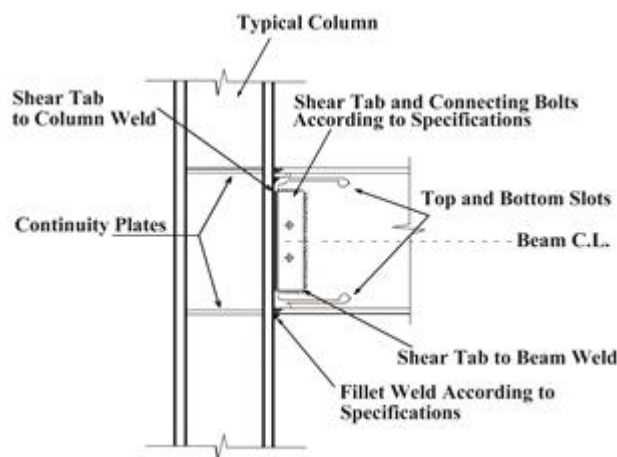


Figure 3. A Typical post-NC

### 2.3.3. A simple illustrative example

A two-story one-bay steel frame structure shown in Fig. 4 is considered to illustrate the implication of consideration of appropriate connection behavior.

The statistical descriptions of all nine random variables in the formulation are summarized in Table 1. It is known to the profession that all random variables may not be equally important for the reliability evaluation. With the help of sensitivity analysis (Haldar and Mahadevan 2000a), some of the less sensitive

random variables can be assumed deterministic at their mean values. This will enhance the computational efficiency. The sensitive random variables considered in this example are also shown in Table 1.

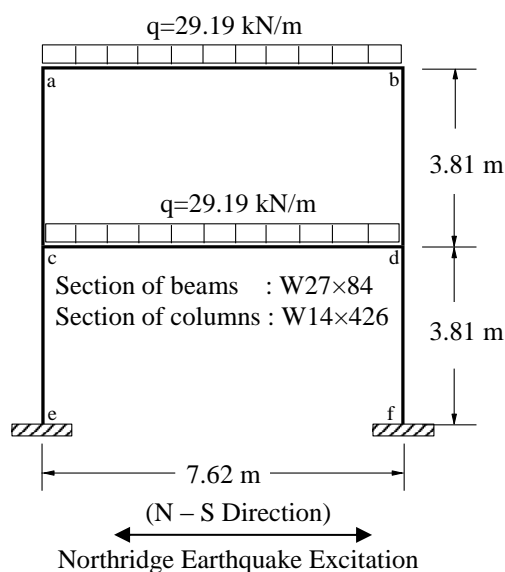


Figure 4. Two-story steel frame structure

Table 1. Statistical description of random variables					
Random Variable	Mean Value	COV	Distribution	Serviceability Limit State	Strength Limit State
$E$ (kN/m <sup>2</sup> )	$1.9994 \times 10^8$	0.06	Ln		
$A^b$ (m <sup>2</sup> )	$1.600 \times 10^{-2}$	0.05	Ln		Deterministic
$I_x^b$ (m <sup>4</sup> )	$1.186 \times 10^{-3}$	0.05	Ln		
$Z_x^b$ (m <sup>3</sup> )	$3.998 \times 10^{-3}$	0.05	Ln	Deterministic	
$A^c$ (m <sup>2</sup> )	$8.065 \times 10^{-2}$	0.05	Ln		Deterministic
$I_x^c$ (m <sup>4</sup> )	$2.747 \times 10^{-3}$	0.05	Ln		
$Z_x^c$ (m <sup>3</sup> )	$1.424 \times 10^{-2}$	0.05	Ln	Deterministic	Deterministic
$F_y$ (kN/m <sup>2</sup> )	$2.4822 \times 10^5$	0.10	Ln	Deterministic	
$\xi$	0.05	0.15	Ln		
$g_e$	1.00	0.20	Type I		

b = beam, c = column

All four beam-to-column connections at  $a$ ,  $b$ ,  $c$ , and  $d$  are considered to be partially restrained. In order to consider the effects of different rigidities in the connections, three  $M-\theta$  curves, denoted as Curve 1,

## Engineering Computations of Large Infrastructures in the Presence of Uncertainty

Curve 2, and Curve 3, shown in Fig. 5, are considered. Curve 1 represents high rigidity, Curve 3 represents very low rigidity, and Curve 2 represents intermediate rigidity. The probabilistic descriptions of the four parameters of the Richard model representing the three curves are listed in Table 2. The frame is excited for 15 seconds by the actual acceleration time history recorded at Canoga Park during the Northridge earthquake of 1994 (North-South component) as shown in Fig. 6. To define the serviceability limit state, the permissible lateral displacement at the top of the frame is assumed to not exceed  $h/400$ , where  $h$  is the height of the frame. Thus, for this example,  $\delta_{allow}$  becomes 1.905 cm, and the corresponding limit state is:

$$g(\mathbf{X}) = \delta_{allow} - y_{max}(\mathbf{X}) = 1.905 - y_{max}(\mathbf{X}) \quad (13)$$

in which  $y_{max}(\mathbf{X})$  is the maximum lateral displacement at the top of the frame. The reliability of the weakest member (beam element c-d) is evaluated for the strength limit state.

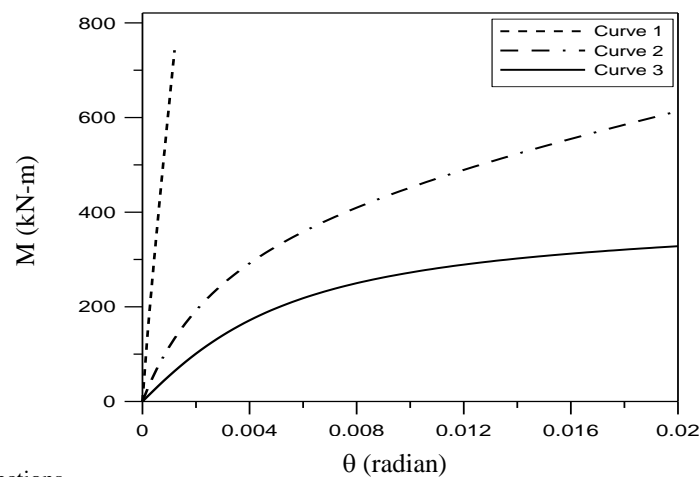


Figure 5. Flexibility of connections

Random variables (1)	Mean Value			COV (5)	Distribution (6)
	Curve 1 (2)	Curve 2 (3)	Curve 3 (4)		
$k$ (kN·m/rad)	$1.13 \times 10^6$	$1.47 \times 10^5$	$5.65 \times 10^4$	0.15	Normal
$k_p$ (kN·m/rad)	$1.13 \times 10^5$	$1.13 \times 10^4$	$1.13 \times 10^3$	0.15	Normal
$M_o$ (kN·m)	508.64	452.12	339.09	0.15	Normal
$N$	0.50	1.00	1.5	0.05	Normal

The reliability indexes of the frame with three different PR connections are estimated and the results are summarized in Table 3. It can be observed that the reliability indexes for the serviceability limit state decreased significantly with the decrease in the rigidity of the PR connections. The frame became very weak in serviceability, particularly when PR connections were represented by very flexible Curve 3. Due to

the redistribution of moment in beam c-d, the reliability indexes for the strength limit state also changed. However, the frame is more prone to failure in serviceability than in strength. This behavior is expected. The consideration of appropriate connection rigidities and the uncertainty associated with modeling them significantly affects the reliability estimation of steel frame structures and cannot be overlooked in any deterministic formulation.

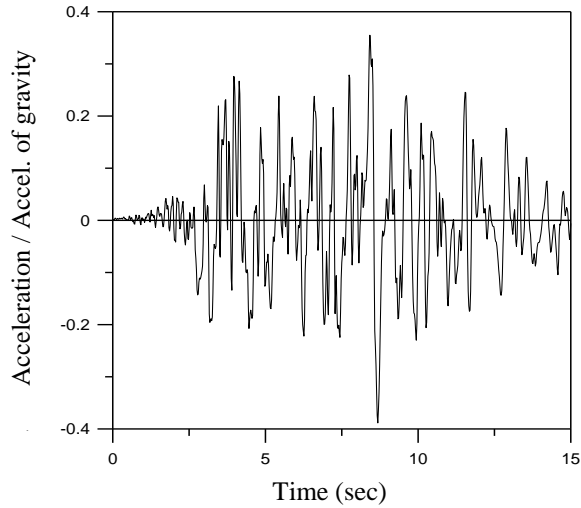


Figure 6. Northridge earthquake time history for 15 seconds (N-S)

Table 3. Reliability indexes with FR and PR connections				
Limit State (1)	FR Connection (2)	PR Connections		
		Curve 1 (3)	Curve 2 (4)	Curve 3 (5)
Serviceability Limit State	$\beta = 1.920$	$\beta_1 = 1.274$	$\beta_2 = -0.008$	$\beta_3 = -0.899$
Strength Limit State Element c-d	$\beta = 3.944$	$\beta_1 = 2.351$	$\beta_2 = 2.558$	$\beta_3 = 3.156$

### 3. Improved SFEM using Computational Sophistication

A robust reliability evaluation technique for large structural systems incorporating all major sources of nonlinearity and uncertainty may not be available at this time. In the presence of such vacuum, one may decide to use simple Monte Carlo simulation (MCS) to address the presence of uncertainty. It is observed by the author that one deterministic analysis of a large structure excited by seismic loading applied in time domain satisfying different sources of energy dissipation and underlying physics may take over 10 hours of computer time. If one decides only say 10,000 cycles of MCS, it will take about 100,000 hours or about 11.4 years of continuous running of a computer. Obviously, it will be impractical.

## Engineering Computations of Large Infrastructures in the Presence of Uncertainty

The basic MCS and SFEM are not realistic alternatives for large structural systems with relatively moderate probability of failure events. The author and his team explored an alternative using the response surface method (RSM) (Box, et al., 1978). The primary purpose of applying RSM in reliability analysis is to approximate the original complex and implicit limit state function using a simple and explicit polynomial (Bucher and Bourgund, 1990; Yao and Wen, 1996; Khuri and Cornell, 1996). Three basic weaknesses of RSM are: (1) it cannot incorporate distribution information of random variables even when it is available, (2) if the response surface is not generated in the failure region, it may not be directly applicable or robust, and (3) for large systems, it may not give the optimal sampling points. Thus, a basic RSM-based reliability method may not be acceptable.

### 3.1. A novel concept

A novel reliability evaluation method is proposed by the author and his team to estimate the reliability of for large structural systems. It is developed in two stages. In the first stage, the two weaknesses of RSM, i.e., the consideration of distributional information of the random variables present in the formulation and identifying the location of the failure region are eliminated by integrating it with FORM/SORM. This approach will lead to a hybrid approach consisting of SFEM, FORM/SORM, and RSM. In the second stage, the efficiency of the method is improved by using several advanced factorial schemes so that the response surface can be generated with fewer sampling points.

#### 3.1.1. Stage 1

Considering the fact that higher order polynomial may result in ill-conditional system of equations for unknown coefficients and exhibit irregular behavior outside of the domain of samples, their utilization in generating RSM, the research team considered second-order polynomial, without and with cross terms for large complicated structural systems. They can be expressed as:

$$\hat{g}(\mathbf{X}) = b_0 + \sum_{i=1}^k b_i X_i + \sum_{i=1}^k b_{ii} X_i^2 \quad (14)$$

$$\hat{g}(\mathbf{X}) = b_0 + \sum_{i=1}^k b_i X_i + \sum_{i=1}^k b_{ii} X_i^2 + \sum_{i=1}^{k-1} \sum_{j>i}^k b_{ij} X_i X_j \quad (15)$$

where  $X_i$  ( $i = 1, 2, \dots, k$ ) is the  $i^{\text{th}}$  random variable, and  $b_0$ ,  $b_i$ ,  $b_{ii}$ , and  $b_{ij}$  are unknown coefficients to be determined. The numbers of coefficient necessary to define Eqs. (14) and (15) are  $p = 2k+1$  and  $p = (k+1)(k+2)/2$ , respectively. The coefficients can be fully defined by estimating deterministic responses at intelligently selected data points called experimental sampling points. The concept behind a sampling scheme can be expressed as:

$$X_i = X_i^C \pm h_i \sigma_{x_i} x_i \quad (16)$$

where  $X_i^C$  and  $\sigma_{x_i}$  are the coordinates of the centre point and the standard deviation of a random variable  $X_i$ , respectively, and  $h_i$  is an arbitrary factor that defines the experimental region.

Sampling points are selected around the center point. The selection of the center point and experimental sampling points around it are crucial factors in establishing the efficiency and accuracy of the proposed

iterative method. The center point is selected to be the coordinates of the checking points as the iteration continues. In the context of iterative scheme of FORM/SORM, the initial center point is selected to be the mean values of the random variable  $X_i$ 's. Then, using the responses obtained from the deterministic FEM evaluations for all the experimental sampling points around the center point, the response surface can be generated explicitly in terms of the random variables  $\mathbf{X}$ . Once a closed form expression for the limit state function is obtained, the coordinates of the checking point can be estimated using FORM/SORM, using all the statistical information on the  $X_i$ 's, eliminating one major deficiency of RSM. The response can be evaluated again at the checking point and a new center point can be selected using linear interpolation from the center point to such that  $g(\mathbf{X}) = 0$  (Huh and Haldar, 2011).

To select experimental sampling points around the center point, saturated design (SD) and central composite design (CCD) are the two most promising schemes. SD is less accurate but more efficient since it requires only as many sampling points as the total number of unknown coefficients to define the response surface. CCD is more accurate but less efficient since a regression analysis is needed to evaluate the unknown coefficients. Also, second-order polynomial with cross terms (Eq. 15) must be used for CCD.

To illustrate the computational effort required for the reliability evaluation of large structural system, suppose the total number of significant random variables, after making some of them deterministic at their mean values, present in the formulation is,  $k = 100$ . The total number of coefficients necessary to define Eq. (14) will be  $2 \times 100 + 1 = 201$  and to define Eq. (15) will be  $(100 + 1)(100 + 2) / 2 = 5151$ . It can also be shown that if Eq. (14) and SD scheme are used to generate the response surface, the total number of sampling points, essentially the total number of deterministic FEM-based time domain nonlinear response analyses will be 201. However, if Eq. (15) and full SD scheme are used, the corresponding deterministic analyses will be 5151. If Eq. (15) and CCD scheme are used, the corresponding deterministic analyses will be  $2^{100} + 2 \times 100 + 1 = 1.2676506 \times 10^{30}$ . Obviously, some of these alternatives may not be meaningful.

Since the proposed algorithm is iterative and the basic SD and CCD require different amount of computational effort, considering efficiency without compromising accuracy, several schemes can be followed. Among numerous schemes considered by the research team, one basic and two promising schemes are: Scheme 0 - SD using 2nd order polynomial without the cross terms throughout all the iterations, Scheme 1- Implement SD using Eq. (14) for the intermediate iterations and SD using Eq. (15) for the final iteration, Scheme 2 – Implement SD using Eq. (14) for the intermediate iterations and CCD using Eq. (15) for the final iteration. This will be discussed in detail during the presentation.

### 3.1.2. Stage 2

Schemes 1 and 2 may be major improvements but still may not be able to estimate the reliability of large structural systems. They may require fewer deterministic evaluations but still they could be in thousands. Their efficiency can be improved significantly by reducing the deterministic evaluations in hundreds in the following way. A conceptual description of the improvement of Scheme 1, denoted as Scheme M1, is discussed very briefly below.

Scheme M1: To improve the efficiency of Scheme 1, the cross terms (edge points),  $k(k-1)$ , are suggested to be added only for the most important variables in the last iteration. Since the proposed algorithm is an integral part of FORM/SORM, all the random variables in the formulation can be arranged in descending order of their sensitivity indexes  $\alpha(X_i)$ . The sensitivity of a variable  $X$ ,  $\alpha(X)$  is the directional cosines of the unit normal vector at the design point. In the last iteration, the cross terms are added only for the most sensitive random variables,  $m$  and the corresponding reliability index is calculated. The total number of

FEM analyses required for Scheme 1 and M1 are  $(k+1)(k+2)/2$  and  $2k+1+m(2k-m-1)/2$ , respectively. For an example, suppose for a large structural system,  $k=100$  and  $m=2$ , the total number of required FEM analyses will be 5151 and 398, respectively, a significant improvement in the efficiency without compromising the accuracy. It will be demonstrated during the presentation with the help of examples.

#### 4. Structural Health Assessment

Structural health assessment (SHA) has become one of the multi-disciplinary challenging research topics all over the world. SHA is an age-old problem. In the past, cracks and cavities were detected in pottery by listening to the sound generated when tapped by fingers, or by hitting structures with a hammer and listening to the sounds they produce, or by conducting simple visual inspection. They are essentially non-model based Non-Destructive Evaluation (NDE) of health of a structure. Several non-model instrument-based techniques were subsequently developed. Their success depends on the knowledge in priori the location(s) and types of defects. For the SHA of large infrastructures, the location(s), types, and severity are expected to be unknown at the time of inspection and thus sophisticated non-model instrument-based techniques are expected to be inapplicable. This led to the development of several model-based approaches. Initially, because of its simplicity, responses produced by static application of loading were measured for SHA. Although computationally more challenging, model-based approaches using dynamic response information has attracted attention of the profession in the recent past. Structural health assessment using dynamic response information has progressed in two fronts: modal information-based and time domain. The general consensus is that modal-based approaches fail to evaluate the health of individual structural elements; they indicate overall effect, i.e., whether the structure is defective or not (Ibanez, 1973; Ghanem and Ferro, 2006). It was reported that even when a member breaks, the natural frequency may not change more than 5%. This type of change can be caused by the noises in the measured responses. Civil infrastructures are expected to have defects, even minor in nature, from the early stage of operation. Identification of locations of defects at the local element level and assessment of their severity are two main objectives of SHA. If defects are large enough to be visible by the naked eye or they change the behavior of structures significantly, no additional effort is necessary. Perhaps it is more critical if the defects are not visible or hidden behind obstructions like fire proofing material.

The author and his team members proposed several novel structural health assessment methods. They are based on the system identification (SI)-based concept and used inverse transformation technique to identify a structure. They represented the structures with the help of finite elements (FEs). The location and severity of defects can be assessed by tracking the changes in the stiffness parameter of each element. Using the information on the current elements' properties, it is straightforward to evaluate the amount or rate of degradation with respect to the "as built" or expected properties, or deviation from the previous values if periodic inspections were conducted. After a repair, it will also indicate the improvement in the structural behavior and whether or not all the defects were repaired.

The basic SI approaches have three components: (1) the excitation, (2) the system to be identified, which can be represented by a series of equations or represented in algorithmic form, e.g., in a FE formulation in terms of mass, stiffness, and damping characteristics of each element, and (3) the output responses caused by the excitation, reflecting the current state of the structure. Using input excitation and output response information, the dynamic properties of all the elements can be evaluated using the inverse algorithm. Simply stated, the numerical values of the dynamic properties of the elements should change to satisfy the response information, reflecting the present physical state of the structure.

### 3.1. Improved engineering computational effort to increase implementation potential

The SI-based concept appears to be simple and straightforward. However, to increase its implementation potential, several advanced computational techniques need to be used.

The governing equation of motion for a multi-degree of freedom (MDOF) structural system with  $ne$  number of elements and  $N$  number of dynamic degrees of freedom (DDOFs) can be written in the matrix form as:

$$\mathbf{M}\ddot{\mathbf{X}}(t) + \mathbf{C}\dot{\mathbf{X}}(t) + \mathbf{K}\mathbf{X}(t) = \mathbf{f}(t) \quad (17)$$

where  $\mathbf{M}$ ,  $\mathbf{K}$ , and  $\mathbf{C}$  are the  $N \times N$  global mass, stiffness, and damping matrices, respectively. They are assumed to be time-invariant for linear structural systems.  $\ddot{\mathbf{X}}(t)$ ,  $\dot{\mathbf{X}}(t)$ , and  $\mathbf{X}(t)$  are the  $N \times 1$  vectors containing measured information on displacement, velocity, and acceleration at all the DDOFs at time  $t$ .  $\mathbf{f}(t)$  is the  $N \times 1$  excitation force vector.

To identify a system, it will necessitate the information on the input excitation as well as the responses (acceleration, velocity, and displacement time histories) at all the dynamic degrees of freedom (DDOFs) must be available to satisfy Eq. (17). However, outside the controlled laboratory environment, the measurement of excitation can be very difficult and thus SHA without excitation information will be very desirable. The author's research team initially proposed a least-squares-based estimation procedure, known as Iterative Least-Squares with Unknown Input (ILS-UI) (Wang and Haldar, 1994). They used viscous-type structural damping. The efficiency of the numerical algorithm was improved later by introducing Rayleigh-type proportional damping, known as Modified ILS-UI or MILS-UI (Ling and Haldar, 2004). Later, Katkhuda et al. (2005) improved the concept further and called it Generalized ILS-UI or GILS-UI. Recently, Das and Haldar (2012) extended the procedure for three dimensional (3D) large structural systems and denoted as 3D GILS-UI.

### 3.2. Limitation of the ILS-UI concept to identify large structural systems

It is practically impossible and uneconomical to measure responses at all DDOFs to apply the basic ILS-UI concept. Responses are expected to be measured only at small parts of large real structural systems for economic reason, to address accessibility problem and without interfering with the normal operating condition. After an extended study, the author's research team concluded that the prediction-correction-based recursive procedures embedded in the extended Kalman filter (EKF) with Weighted Global Iteration (WGI) concept would be appropriate when measured responses were limited. However, to implement the EKF-WGI concept, two additional conditions must be satisfied. First, to satisfy the governing equation of motion, the excitation information must be known, defeating the basic objective of SHA without using excitation information. Second, the initial value of the state vector must be known to start the local iteration. The research team proposed a two-stage substructure approach to mitigate it (Wang and Haldar, 1997).

### 3.3. Structural identification using limited noise-contaminated response information

The health of a large structural system must be assessed using measured dynamic responses. Responses measured even by smart sensors are always expected to be noise contaminated. Thus, in spite of using sophisticated mathematical algorithm, it may not be possible to identify a structure without addressing noise-contamination problems in the response information. In fact, Maybeck (1979) concluded that it was

not possible. There are three basic reasons for his conclusion: (i) no mathematical model to represent a system is perfect, (ii) dynamic systems are not only driven by control inputs, but there are always disturbances that cannot be controlled and modeled deterministically, and (iii) responses observed by sensors do not exhibit the actual perfect system responses, since sensors always introduce their own system dynamics and distortion into measured data. The author and his team had to overcome several challenges of different kinds. The team used that the Kalman filter-based algorithms to identify a system using limited noise contaminated responses and without using excitation information. They conducted comprehensive theoretical and experimental investigations to address them and demonstrated that Maybeck was wrong in making the conclusion. Some of their works are discussed in the following sections.

### 3.4. Kalman filter-based algorithms

In a mathematical sense, the basic KF is a non-deterministic, recursive computational procedure to provide best estimate of the states by minimizing the mean of squared error for a process governed by linear stochastic differential equation. Kalman filter (1960) is very powerful in several ways. It incorporates (i) the knowledge of the system and (ii) statistical information on the system noises, measurement errors and uncertainty in the dynamic models. Since it is a prediction-correction-based procedure, it also requires information on the initial conditions of the variables of interest. They are generally modeled as Gaussian random variables with assigned mean values and covariances.

Since some of the measured responses can be mildly nonlinear, the team used Extended Kalman filter (EKF) in developing the new procedures. To implement the EKF algorithm for structural health assessment using minimum number of noise-contaminated responses without excitation information, the research team proposed a two-stage approach. In the Stage 1, considering the location of input excitation and the available responses, the substructure(s) are selected. Then, the ILS-UI procedure is used to identify the stiffness and damping parameters of all the elements in the substructure(s) and the unknown input excitation. The information obtained in Stage 1 is then used to identify the whole structures in Stage 2. In this way, the health of the whole structure is assessed using only limited number of noise-contaminated responses.

It is not possible to present here the mathematics of the concept. The concept was initially denoted as ILS-EKF-UI. Later, it was improved and denoted as Modified ILS-EKF-UI or MILS-EKF-UI (Ling and Haldar, 2004) and Generalized ILS-EKF-UI or GILS-EKF-UI (Wang and Haldar, 1997). The most up-to-date version of the concept is known as 3D GILS-EKF-UI (Das and Haldar, 2012), developed for general three dimensional structures. Interested readers can obtain necessary information from these publications.

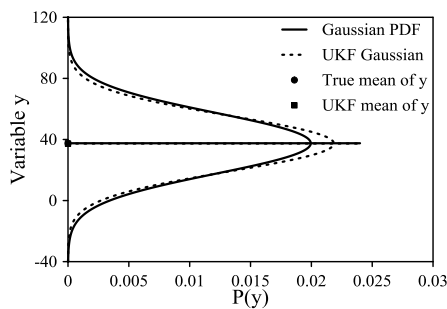
### 3.5. Nonlinear System Identification – Unscented Kalman Filter

The basic KF is essentially applicable for linear structural behavior. For SHA of large structures, the behavior may not be linear. Presence of defects may also cause nonlinearity, even when the excitation is at the low level. This led to the development of the extended Kalman filter (EKF) concept (Hoshia and Saito, 1984). The EKF estimates the state through linearization of the process and measurement equations about the current states and covariances. For highly nonlinear systems, the linearization process in EKF may produce significant error. This prompted the authors to develop UKF-UI (Al-Hussein and Haldar, 2013).

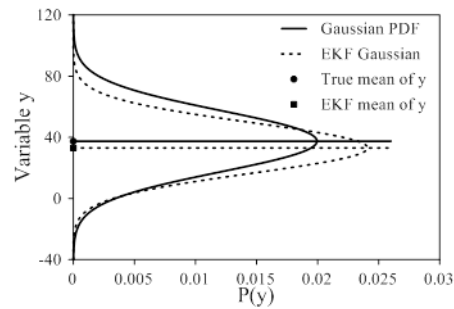
Responses obtained for large structures are expected to be nonlinear. The widely used EKF approach provides only an approximation to the optimal nonlinear estimation. It introduces two major drawbacks. First, the Jacobian matrices need to be derived for linearization. Second, the filter can be unstable if the

sampling interval of the measured responses is not sufficiently small. The UKF method was introduced to remove both shortcomings (Julier, et al., 1995). The main idea of UKF is to generate several sampling points (sigma points) around the current state estimate based on its covariance. Then, these points are explicitly propagated through the nonlinear system equations to get more accurate estimation of the mean and covariance of the mapping results. Suppose, a nonlinear function  $y = e^x$  and  $x$  is a Gaussian random variable with a mean of 3.5 and a variance of 0.25. The true mean and variance of  $y$  can be calculated as 37.52 and 399.94, respectively. The corresponding mean and variance of  $y$  according to UKF are found to be 37.34 and 333.50, respectively, and according to EKF are 33.12 and 274.16, respectively, indicating the errors in the estimation using the two procedures.

The propagations of uncertainties using UKF and EKF are shown in Fig. 7. It can be observed that the UKF approximates the propagation of the uncertainty in terms of the probability density function in the presence of large nonlinearity more accurately than the EKF (Al-Hussein and Haldar, 2013).



(a) Gaussian PDF of  $y$  using UKF



(b) Gaussian (PDF) of  $y$  using EKF

Figure 7. Propagation of uncertainties using UKF and EKF

## 5. Data Analysis Challenges

The structural health assessment procedures discussed above required very sophisticated engineering computations including severe level of nonlinearities. However, their implementation required measured response information. As mentioned earlier, measured responses are always noise-contaminated. And the SI-based algorithms will fail to assess structural health if uncertainty in the measured responses is not mitigated appropriately. Thus, reliable computation must be conducted in the presence of uncertainty. It is a very difficult task. Some of the major issues are very briefly discussed in the following sections.

### 5.1 Post-Processing of the Accelerometer Data

To implement all the structural health assessment procedures discussed above, acceleration time histories must be measured at the substructure(s). A raw acceleration time-history may contain many sources of errors, including noises, high frequency content, slope, and DC bias, as shown in Fig. 8. Since acceleration time-histories are needed to be successively integrated to generate velocity and displacement time histories in the proposed methods, post-processing of measured acceleration time histories are required to remove the sources of error (Vo and Haldar, 2003).

The first step in post-processing the raw data was to convert from millivolts to acceleration unit ( $m/s^2$ ) by multiplying the accelerometer raw data with the calibrated scale factor supplied by the manufacturer.

Next, an eighth order Butterworth low-pass filter was applied to the normalized data with a cutoff frequency (120 Hz used in the study). Then, the data was normalized about the zero mean to remove the DC bias and the integration error. The velocity and displacement time-histories were then obtained by integrating the filtered acceleration data twice; after each integration operation, a second order low-pass filter with a cut off frequency at 10 Hz was applied to the data. This is necessary to remove the integration residual errors. Without the low-pass filter, the response velocity and displacement will not be symmetric.

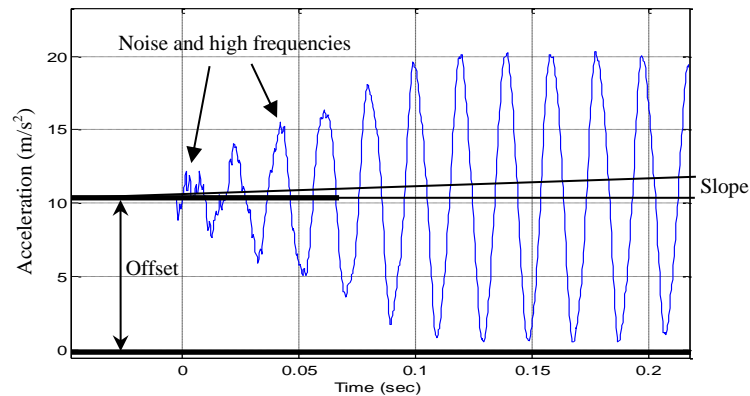


Figure 8. Measured acceleration time-history

## 5.2 Mitigation of Noise, Amplitude, and Phase-Shift Errors

It is important to note that the proposed methods failed to converge even after implementing all the post-processing techniques discussed above. Unlike noise, amplitude and phase-shift errors generally cannot be detected from the plotting of the acceleration time-histories in normal scales and is generally overlooked.

### 5.2.1. Noise

When numerically generated noise-contaminated responses were used to predict the structural health, the algorithm successfully predicted the element stiffness properties for both noise-free and noise-contaminated responses. This eliminates noise as the main cause of non-convergence, removing one of the myths.

### 5.2.2 Amplitude Error

Amplitude or cross coupling error, as shown in Fig. 9, is primarily caused by mechanical misalignments of the sensing element mounted inside the accelerometer's case. It is one of the major reasons of non-convergence. The amplitude error can be mitigated by using fewer nodal responses (Vo and Haldar, 2004; Haldar et al., 2013).

### 5.2.3 Phase-Shift Error

There are two separate sources of error that cause relative phase-shift in the measured responses, as shown in Fig. 10. The primary source of phase-shift error is the integration of the measured acceleration. The second source of phase-shift error is data latency caused by the sampling rate of the data logger. This error occurs because there is a time delay in the sampling of two consecutive responses. The phase shift error was mitigated by scaling the responses of all nodes in the finite element representation using the transverse response of a single reference node (Vo and Haldar, 2004; Haldar et al., 2013).

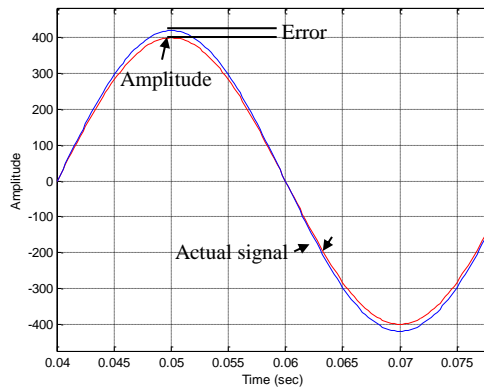


Figure 9. Amplitude error

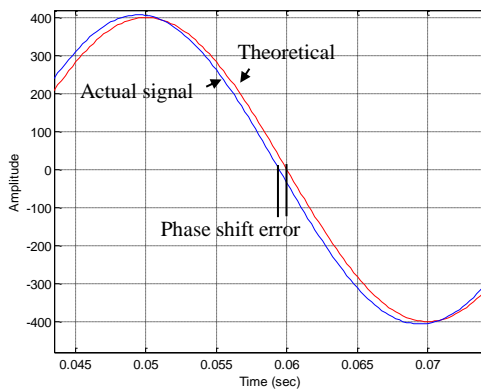


Figure 10. Phase-shift error

### 5.3. Modeling of Structures and Selection of Substructures

It is widely known that the measured responses do not match with analytical results. Also, a structure tested during one inspection may not remain the same during the next inspection. Commonly used data processing techniques discussed earlier may not be sufficient to address the related issues. Based on their extensive experience from laboratory investigations, the team observed that one of the major reasons for the discrepancy is that structural properties of the elements used in the mathematical formulation and in reality are not the same (Martinez-Flores and Haldar, 2007). It will be discussed in detail during the presentation.

### 5.4. Size and Numbers of Substructures

The success of the proposed procedures using the substructure approach with minimum response information will depend on the location, size and numbers of the substructure used. A substructure is a small part of a structure that satisfies all the requirements to implement the GILS-UI procedure. Katkhuda and Haldar (2008) suggested how to select substructure(s) based on the available measured response

## Engineering Computations of Large Infrastructures in the Presence of Uncertainty

information. The size of the substructure should be kept to an absolute minimum for economic reason. However, the defect predictability improves significantly when the defect is located within or close to the substructure. Multiple substructures may be necessary for large structures since at least one of them will be closer to the location of defect (Haldar et al., 2013).

### 6. Conclusions

Engineering computation capability has advanced exponentially in recent years. Increased computer power is one of the major reasons for this growth. Although the simulation-based computations have increased significantly in the recent past to address uncertainty-related problems, their applications to study realistic behavior of large infrastructures are limited. The first part of the paper presents the incorporation of uncertainty in a finite element-based computational formulation, denoted as the stochastic finite element method. The concept is improved further by combining sensitivity analysis, model reduction techniques, efficient response surface method-based sampling schemes, and several advanced factorial schemes producing compounding beneficial effect to obtain efficiency without sacrificing accuracy. It is discussed in the second part. In the third part, sophisticated computation schemes are integrated with noise-contaminated measured response information to extract features of practical interest in the context of structural health assessment. The uncertainty in the measured data cannot completely be eliminated, but measured response data are needed to be integrated with advanced computational schemes for the maximum benefits. In the late 1970s it was erroneously concluded that such integration was not possible.

### Acknowledgements

The author would like to thank all the team members for their help in developing several research concepts presented here. It will be impractical to identify all of them here. The team received financial supports from the National Science Foundation, a small grant from the University of Arizona, graduate student supports from various sources including Raytheon Missile Corporation, Ministry of Higher Education, Jordon, CONACYT, Iraq's Ministry of Higher Education and Scientific Research, Department of Civil Engineering and Engineering Mechanics, University of Arizona, etc. Any opinions, findings, or recommendations expressed in this paper are those of the author and do not necessarily reflect the views of the sponsors.

### References

- Al-Hussein A, and Haldar A, A Novel Unscented Kalman Filter for Health Assessment of Large Structural Systems with Unknown Input, *ASCE J. Eng. Mech.* (2013), (under review).
- Al-Hussein A, Das A K, and Haldar A, A New Approach for Structural Health Assessment Using Unscented Kalman Filter, *11th Int. Conf. on Structural Safety and Reliability (ICOSSAR'13)*, Columbia University, New York, N.Y. (2013).
- Box, G. P., William G. H., and Hunter, J. S. (1978), *Statistics for Experimenters: An Introduction to Design, Data Analysis and Modeling Building*, John Wiley & Sons, New York, N.Y.
- Bucher, C.G. and Bourgund, U. (1990), A fast and efficient response surface approach for structural reliability problems, *Structural Safety*, 7, 57-66.
- Colson, A. (1991), Theoretical modeling of semirigid connections behavior, *J. of the Construction steel Research*, 19, 213-224.
- Das A K, and Haldar A, Health Assessment of Three Dimensional Large Structural Systems – A Novel Approach, *Life Cycle Reliability and Safety Eng.* (2012), Vol 1, No 1, pp 1-14.
- El-Salti, M. K. (1992), *Design of frames with partially restrained connections*, Ph.D. Dissertation, Dept. Of Civil Engineering and Engineering Mechanics, University of Arizona.

- Federal Emergency Management Agency (FEMA). (2000). Seismic Design Criteria for Steel Moment-Frame Structures, FEMA 350-353 and 355A-F.
- Ghanem, R. and Ferro, G. (2006). Health Monitoring For Strongly Non-Linear Systems Using the Ensemble Kalman Filter, *Struct. Control and Health Monitoring*, 13, 245-259.
- Haldar A, Das A K, and Al-Hussein A. (2013). Data Analysis Challenges in Structural Health Assessment using Measured Dynamic Responses, *Advances in Adaptive Data Analysis*, 5(4), 1-22.
- Haldar, A. and Gao, L. (1997), Reliability evaluation of structures using nonlinear SFEM, Uncertainty Modeling in Finite Element, Fatigue, and Stability of Systems, edited by A. Haldar, A. Guran, and B.M. Ayyub, World Scientific Publishing Co., 23-50.
- Haldar, A. and Mahadevan, S. (2000a), *Probability, Reliability And Statistical Methods In Engineering Design*, John Wiley & Sons, New York, N.Y.
- Haldar, A. and Mahadevan, S. (2000b). *Reliability Assessment Using Stochastic Finite Element Analysis*, John Wiley & Sons, NY.
- Haldar A, Martinez-Flores R, and Kathuda H. (2008). Crack Detection in Existing Structures Using Noise-Contaminated Dynamic Responses, *Theoretical and Applied Fracture Mechanics*, 50(1), 74-80.
- Hoshiya M, and Saito E. (1984). Structural Identification by Extended Kalman Filter, *ASCE J. Eng. Mech.* 110(12), 1757-1770.
- Huh, J. and Haldar, A. (2001), Stochastic Finite-Element-Based Seismic Risk of Nonlinear Structures. *Journal of Structural Engineering, ASCE*, 127(3), 323-329.
- Huh, J., And Haldar, A. (2011). A Novel Risk Assessment Method for Complex Structural Systems. *IEEE Transactions on Reliability*, 60(1), 210-218.
- Ibanez, P. (1973). Identification of Dynamic Parameters of Linear and Non-Linear Structural Models from Experimental Data, *Nucl. Eng. and Design*, 25, 30-41.
- Julier S J, Uhlmann J K, and Durrant-Whyte H F. (1995). A New Approach for Filtering Nonlinear Systems, *Proc. of the American Control Conf.*, Seattle, Washington, 1628-1632.
- Kalman R E, A New Approach to Linear Filtering and Prediction Problems, *Trans. of the ASME-J. Basic Eng.* (1960), pp 35-45.
- Kathuda H, and Haldar A. (2008). A Novel Health Assessment Technique with Minimum Information, *Struct. Cont. & Health Monitoring* (2008), Vol 15, No 6, pp 821-838.
- Kathuda H, Martinez-Flores R, and Haldar A, Health Assessment at Local Level with Unknown Input Excitation, *ASCE J. Struct. Eng.*, 131(6), 956-965.
- Khuri, A. I. and Cornell, J. A. (1996), *Response Surfaces Designs and Analyses*, Marcel Dekker, New York, N.Y.
- Kim, S. H. and Na, S. W. (1997), Response surface method using vector projected sampling points, *Structural Safety*, 19(1), 3-19.
- Ling X, and Haldar A. (2004). Element Level System Identification with Unknown Input with Rayleigh Damping, *ASCE J. Eng. Mech.*, 130(8), 877-885.
- Lucas, J. M. (1974), Optimum Composite Designs, *Technometrics*, 16(4), 561-567.
- Martinez-Flores R, and Haldar A. (2007). Experimental Verification of A Structural Health Assessment Method without Excitation Information, *J. Struct. Eng.*, 34(1), 33-39.
- Maybeck, P S. (1979). *Stochastic Models, Estimation, and Control Theory*, Academic Press, Inc.
- Rajashekhar, M.R. and Ellingwood, B. R. (1993), A new look at the response surface approach for reliability analysis, *Structural Safety*, 12, 205-220.
- Richard, R. M. and Abbott, B.J. (1975), Versatile elastic-plastic stress-strain formula. *Journal of Engineering Mechanics, ASCE*, 101(EM4), 511-515.
- Richard, R.M. Allen, C.J. and Partridge, J. E. (1997). Proprietary slotted beam connection designs, *Modern Steel Construction*, Chicago, Illinois.
- Richard, R. M. and Radau, R. E. (1998). Force, stress and strain distribution in FR bolted welded connections, *Proceedings of Structural Engineering Worldwide*.
- Vo P H, and Haldar A. (2003). Post Processing of Linear Accelerometer Data in System Identification, *J. Struct. Eng.*, 30(2), 123-130.
- Vo P H, and Haldar A. (2004). Health Assessment of Beams - Theoretical and Experimental Investigation, *Advances in Health Monitoring/Assessment of Structures including Heritage and Monument Structures, J. Struct. Eng.*, 31(1), 23-30.
- Wang D, and Haldar A. (1994). An Element Level SI with Unknown Input Information, *ASCE J. Eng. Mech.*, 120(1), 159-176.
- Wang D, and Haldar A. (1997). System Identification with Limited Observations and without Input, *ASCE J. Eng. Mech.*, 123(5), 504-511.
- Yao, T. H.-J. and Wen, Y.K. (1996). Response surface method for time-variant reliability analysis, *Journal of Structural Engineering, ASCE*, 122(2), 193-201.